Mechanical Properties of Ethylene–Vinyl Acetate/Polystyrene Blends Studied by *In Situ* Polymerization

Shih-Kai Cheng,[1] Po-Tsun Chen,[1] Cheng-Chien Wang,[2] Chuh-Yung Chen[1]

[1]*Department of Chemical Engineering, National Cheng-Kung University, Tainan, Taiwan 70101*
[2]*Department of Chemical Engineering, Southern Taiwan University of Technology, Tainan, Taiwan 710*

Received 4 December 2001; accepted 15 May 2002
Published online 11 February 2003 in Wiley InterScience (www.interscience.wiley.com). DOI 10.1002/app.11667

ABSTRACT: This study examined ethylene–vinyl acetate (EVA)-toughened polystyrene (PS). EVA is well-known to be incompatible with PS; thus, the PS graft to the EVA backbone (EVA-*g*-PS) was used as a compatibilizer and provided good adhesion at the interface of PS and EVA. In addition, the mechanical properties and impact resistance of the PS matrix were obviously improved by EVA-*g*-PS and by EVA itself. Meanwhile, differential scanning calorimetry results showed that the grafted PS chain influenced the crystallization of EVA; for example, the melting temperature, the crystallization temperature, and the percentage crystallinity related to EVA were reduced. Moreover, the addition of 10% EVA increased the impact strength by a factor of five but reduced the modulus by the same factor. Additionally, a lower number-average molecular weight EVA delayed phase inversion and resulted in poor mechanical properties. A fracture surface photograph revealed that the major mechanism of EVA-toughened PS was craze and local matrix deformation. © 2003 Wiley Periodicals, Inc. J Appl Polym Sci 88: 699–705, 2003

Key words: blends; fracture; mechanical properties

INTRODUCTION

Polystyrene (PS) toughened by the addition of rubber was studied early, in the 1920s. Early developments involved high-impact polystyrene (HIPS), launched by Dow Chemical, which was accomplished with polybutadiene rubber (PB), according to the works reviewed by Amos et al.[1] and Pohlemann and Echte.[2] In this process, PB can be dissolved in styrene monomer (SM), which results in *in situ* radical polymerization. During the polymerization, both PS homopolymer and PS grafted to PB copolymer are simultaneously formed. Thus, the graft copolymer acts as an emulsifier or compatibilizer to improve the interaction between the PS and PB phases. However, the PB/SM mixture inverts into dispersed particles and forms a salami structure in the PS matrix after further polymerization. Transmission electron microscopy was used to discover the salami structure[3] and to explain the toughening mechanism. The salami structure consists of PB particles within PS subinclusions; however, this can effectively increase the toughening volume of PB. Thus, only a little PB (5–10%)[4] is required to toughen PS.

HIPS and acrylonitrile–butadiene–styrene (ABS) copolymer are well-known commercial products and are widely used in electronic products. Unfortunately, both HIPS and ABS have serious problems that are caused by the unsaturated bonds of PB. Process temperatures above about 250°C cause excessive thermal oxidation in the unsaturated bonds of PB. Therefore, we considered saturated elastomers[5] considered as replacements for PB for the toughening of PS.

Ethylene–vinyl acetate (EVA) elastomer is a suitable material for toughening PS because all of the chemical chain of EVA is saturated. In studies of PS toughening that used EVA,[6–8] the mechanical blend caused larger rubber particles, which resulted in poorer toughness. The use of a graft copolymer blend provides a great dispersion of rubber particles and improves the miscibility of the mixture. Although Barbosa and colleauges[9,10] successfully controlled the grafting level and the number-average molecular weight (M_n) of the grafted PS, the process used was too complicated. In this study, we used *in situ* radical graft copolymerization for a simpler manufacture of EVA-toughened PS. Because graft polymerization with peroxide radicals is more efficient than that of azo radicals,[11–16] a peroxide initiator was used to induce the graft copolymerization and to improve the toughness of PS.

Correspondence to: C.-Y. Chen (ccy7@ccmail.ncku.edu.tw or comet127@ms34.hinet.net).

Contract grant sponsor: National Science Council of the Republic of China; contract grant number: NSC 89-2216-E-006-057.

TABLE I
Recipe for the EVA-Toughened PS Sheet

Sample[a]	EVA (wt %)	EVA (g)	SM (g)	*t*-BO (g)[b]	BPO (g)[b]
MIL1	1	10	990	1.21	0.59
MIL3	3	30	970	1.19	0.58
MIL6	6	60	940	1.15	0.56
MIL10	10	100	900	1.10	0.54
MIH1	1	10	990	1.21	0.59
MIH3	3	30	970	1.19	0.58
MIH6	6	60	940	1.15	0.56
PS	0	0	1000	1.23	0.60

[a] MIL: VA content = 18%, MI = 0.7; MIH: VA content = 18%, MI = 2.5.
[b] *t*-BO/BPO (by molar ratio) = 7/3.

EXPERIMENTAL

Preparation of the EVA-toughened PS sheet

SM (commercial grade, purified by distillation) was added to a Pyrex reactor and mixed with two kinds of EVA copolymer [vinyl acetate (VA) content = 18%, melt flow index (MFI) = 0.7; VA content = 18%, MFI = 2.5]. All EVAs were purified by Soxhlet extraction to remove additives and mixed with SM at 85°C until the EVA dissolved. Polymerization proceeded after the addition of a *tert*-butyl peroctoate (*t*-BO)/benzoic peroxide (BPO) mixture, according to the specifications in Table I. When the polymerization reached an appropriate viscosity, the prepolymer solution was cast into a mold made of two tempered glasses, with poly(vinyl chloride) packing around the glass. The mold was moved to an 80°C water bath for 20 h and was then cured at 100°C in an oven for 1 h. The toughened PS sheet was available after the mold was cooled.

Grafting level

EVA-*g*-PS and PS in copolymer were separated by the demixing method. A methyl cyclohexane (MCH; 150 g)/dimethylformamide (DMF; 50 g) mixture was prepared in a flask, and 0.5 g of the casting product was added at 90°C. After the sample completely dissolved and cooled, the solution was separated for 1 day by gravity. The upper layer was the turbid solution of EVA-*g*-PS/MCH; the lower layer was the clear PS/DMF solution, as presented in Scheme 1. Both layers were dried and weighed; the grafting level was calculated as follows:

$$\text{Grafting level} = \frac{\text{amount of grafted PS}}{\text{amount of EVA}} \times 100\%$$

Mechanical tests

A casting sheet was cut into a rectangle and grooved with a rotating knife into a dumbbell shape (ASTM D 638, Type I). Tensile tests were performed on a universal testing machine (Instron 1101) at a constant crosshead speed of 5 mm/min. The Izod impact resistance of V-notched samples was obtained with a standardized pendulum impact testing machine. The bar dimensions were 65 × 13 × 3 mm. The fracture surface was examined by scanning electron microscopy (SEM).

RESULTS AND DISCUSSION

Effect of grafted PS

MCH and DMF were immiscible at room temperature but formed a homogenous mixture above 60°C. EVA-*g*-PS/PS dissolved at 90°C; the mixture could be separable after cooling because EVA did not dissolve in DMF at room temperature. The lower layer consisted of PS/DMF because it was homogeneous, and the upper layer was an EVA-*g*-PS/MCH turbid solution. The composition of each layer was analyzed with an elementary analyzer, and the grafting level is shown on Table II.

We used differential scanning calorimetry (DSC) to analyze the dried products of both layers. A comparison with the pure EVA is shown in Table II; melting temperature (T_m), and crystallization temperature (T_c) of the grafted copolymers decreased with grafting

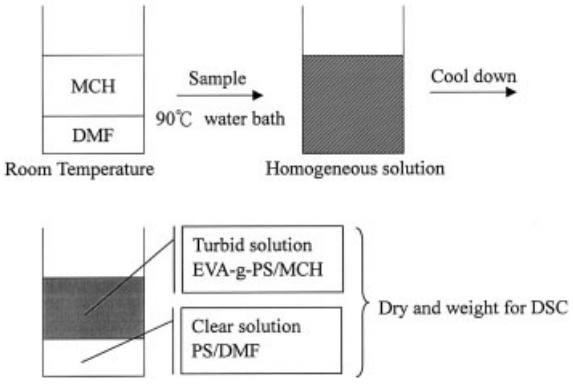

Scheme 1 Demixing method procedure.

TABLE II
Summary of the Grafting Levels and DSC Results After Demixing Separation

		EVA-PS		
	EVA	MIL1	MIL6	MIL10
Grafting level (%)		426	163	46
T_m (°C)	88.0	83.4	85.9	87.0
ΔT_m (°C)		−4.6	−2.1	−1.0
T_c (°C)	65.7	43.9	46.8	63.0
ΔT_c (°C)		−21.8	−18.9	−2.7
ΔH_f (J/g)				
Experimental	60.37	5.10	15.21	39.35
Theoretical		11.48	22.95	41.35
ΔH_c (J/g)				
Experimental	63.57	5.02	17.49	39.84
Theoretical		12.09	24.17	43.54
Relative X_c[b] (%)		44	66	95

[a] Theoretical ΔH was calculated from ΔH of pure EVA, with the weight percentage of EVA in the EVA-*g*-PS taken into account.

[b] X_c = Percentage crystallinity related to EVA content in EVA-*g*-PS. X_c = Experimental ΔH_f/Theoretical $\Delta H_f \times 100\%$.

level. The results indicate that the grafted PS chain exhibited some influence on the crystallinity of EVA. From grafting level and DSC results, the heat of fusion (ΔH_f) and the heat of crystallization (ΔH_c) of EVA-*g*-PS could be compared with those of pure EVA, and we determined the relative percentage crystallinity (X_c) of EVA-*g*-PS. The more PS grafted onto the EVA, the less crystalline structure was formed, which indicates that the grafted PS chain indeed affected EVA crystallinity.

Mechanical test results

Table III and Figures 1 and 2 present the results of tensile tests, Izod tests, and the fracture surface morphologies of the EVA-toughened PS, respectively. Impact strength and elongation were obviously improved by the addition of the amount of EVA. Notably, the impact strength of sample MIL10 was higher than PS by about five times and the elongation by about six times, but the modulus was approximately halved. In addition, the toughened fracture surface was rougher than that of PS, and the roughness increased with the amount of EVA, as shown in Figures 1 and 2. When the EVA concentration was 1% (MIL1), the size of the dispersed phase of EVA was located in the range of 3–5 μm, and the PS subinclusions were enclosed within the EVA phase, as shown in Figure 3. Restated, the salami structure of EVA in the PS matrix was formed at low EVA concentrations. That salami structure should have been introduced from the graft copolymer formed near the PS and EVA phases during polymerization. The 426% grafting level was too high to prevent the trapped SM in the EVA phase from diffusing outward. Many PS subinclusions were located in EVA phase and resulted in the dispersed volume of EVA being larger than the actual volume of the added EVA.[17] However, the EVA-*g*-PS copolymer also improved the adhesion between the PS and EVA phases, which greatly benefitted the impact strength and elongation of EVA-toughened PS. An obvious yielding occurred in MIL6 and MIL10, as shown in Figure 4(a). Table III shows that the impact strength and the elongation of MIL6 and MIL10 were much higher than MIL1. Furthermore, the SEM photographs of the fracture surface revealed serious deformation of the PS matrix around the dispersed phase in MIL6 and MIL10. Additionally, the EVA dispersed phase could act as an energy absorption site because the EVA phase also deformed during the mechanical tests. Therefore, the presence of the grafted copolymer in the interface not only improved the adhesion of EVA particles and the PS matrix, preventing the particles from being pulled out of the matrix, but also enabled them to act as stress-transfer agents when external stress was applied.

However, elongation of the EVA-toughened PS increased with the EVA concentration. A lot of crazes were induced, as shown in the SEM of the fracture surface; meanwhile, the stress whitening was also more serious because these crazes existed in the stress-whitening region. Both the specimen volume and the elongation increased with the EVA concentration, but the modulus and yielding stress decreased as EVA concentration increased. The modulus and yielding stress were much lower than those of PS because EVA is an elastomer. The more EVA there was enclosed within PS matrix, the lower was the modulus of the toughened PS. In research on HIPS,[17–19] when an external stress was applied to the specimen, the rubber particles first concentrated stress and then initiated craze because of their low moduli. Yielding also indicated the forming of craze. The PS matrix deformed after craze formation. The low yielding stress for EVA/PS material implies that the craze could be induced under low external stress. The experiment showed that yielding stress decreased as EVA concentration increased. Because the distance between dispersed particles was shorter at higher EVA concentrations, the overlapping stress fields of the particles increased stress concentration at the EVA surface and, thus, promoted the yielding of the specimen. Figure 4

TABLE III
Results of Tensile and Izod Impact Tests

	PS	MIL1	MIL3	MIL6	MIL10
Modulus (MPa)	1300	1030	960	840	680
Tensile strength (Mpa)	29.5	28.9	28.9	22.8	21.4
Elongation (%)	2.5	3.8	4.4	8.5	15.0
Impact strength (KJ/mm^2)	2.9	3.5	3.5	11.7	14.6

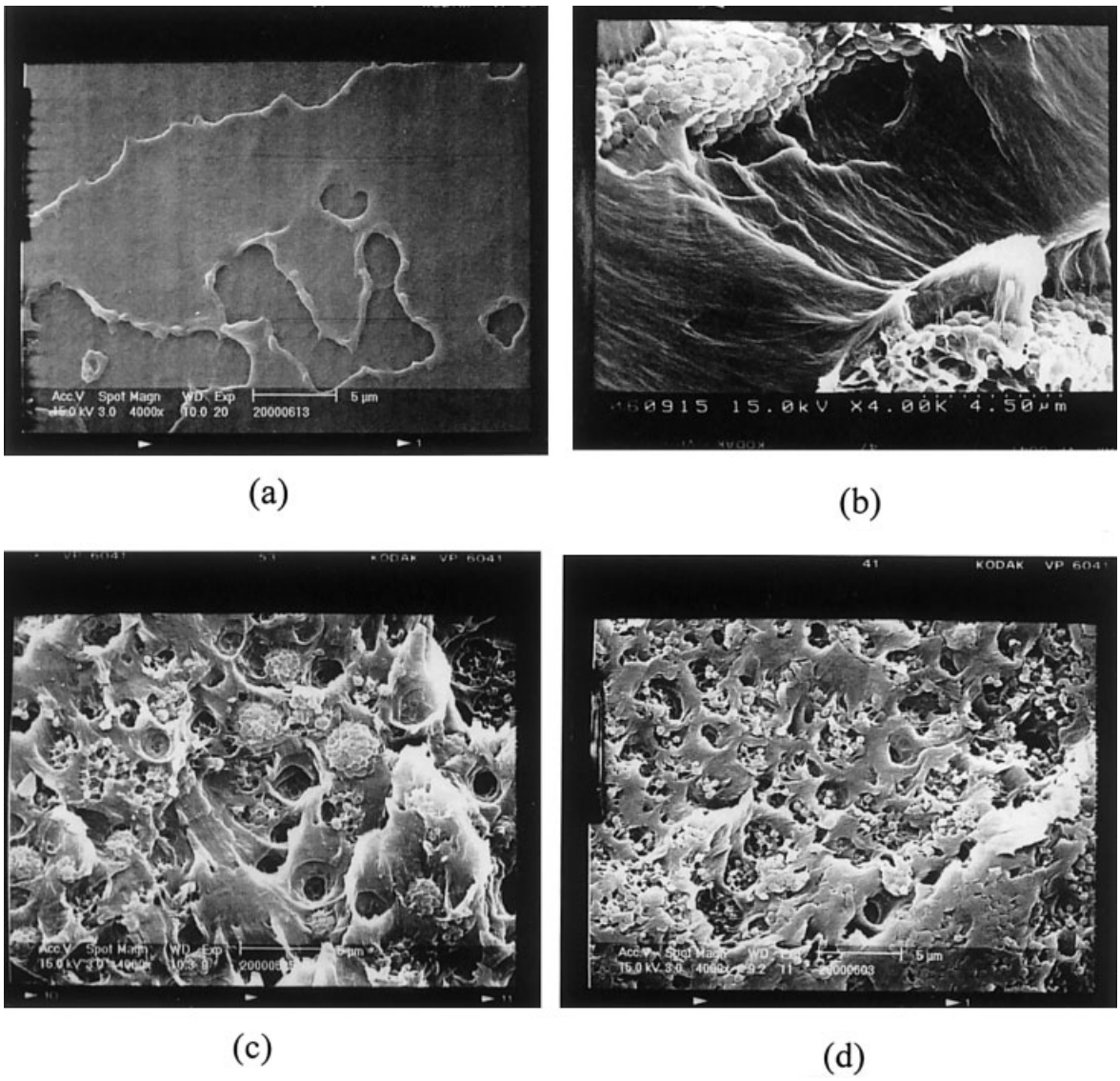

Figure 1 SEM photographs of the fracture surface by the tensile test: (a) PS, (b) MIL1, (c) MIL6, and (d) MIL10.

shows the relationship between yielding stress and EVA fraction.

The stress did not decrease after yielding in MIL1 (Fig. 4). On the contrary, stress decreased after yielding in MIL6 and MIL10. According to the photograph of the fracture surface, less craze was induced in MIL1 because the volume fraction of the EVA phase was smaller. However, MIL6 and MIL10 induced a large amount of craze during yielding and responding to reduce their stress. Consequently, an obvious yielding point was observed in MIL6 and MIL10.

Effect of the molecular weight of EVA

The MFI of the polymer was affected by additives, molecular weight, chemical properties, and so on. The EVAs were purified to remove the additives, and the MFI was about the same before and after purification. Thus, the MFI was related to the molecular weight. In this study, EVA-toughened PS with a higher MFI and the same VA content was used to elucidate the effect of the molecular weight (M_n) of EVA (MIH1, MIH3, MIH6). A large molecular weight of EVA corresponded to low MFI. The results of tensile strength tests (Fig. 4) and Izod impact strength tests (Fig. 5) in a variety of MFIs for the EVA-toughened PS matrix showed poor toughness with lower M_n (higher MFI). Because M_n is directly proportional to viscosity, the higher viscosity provides a higher shear force then the lower one. During the polymerization, this is a benefit for the dispersion of the particles. According to the thermodynamic theorem, a polymer with a lower M_n in the mixture causes a larger entropy change of mixing, enhancing the solubility of the polymer.[20] Therefore, EVA with a low M_n more easily dissolved in SM. The single-phase region was, therefore, enlarged in

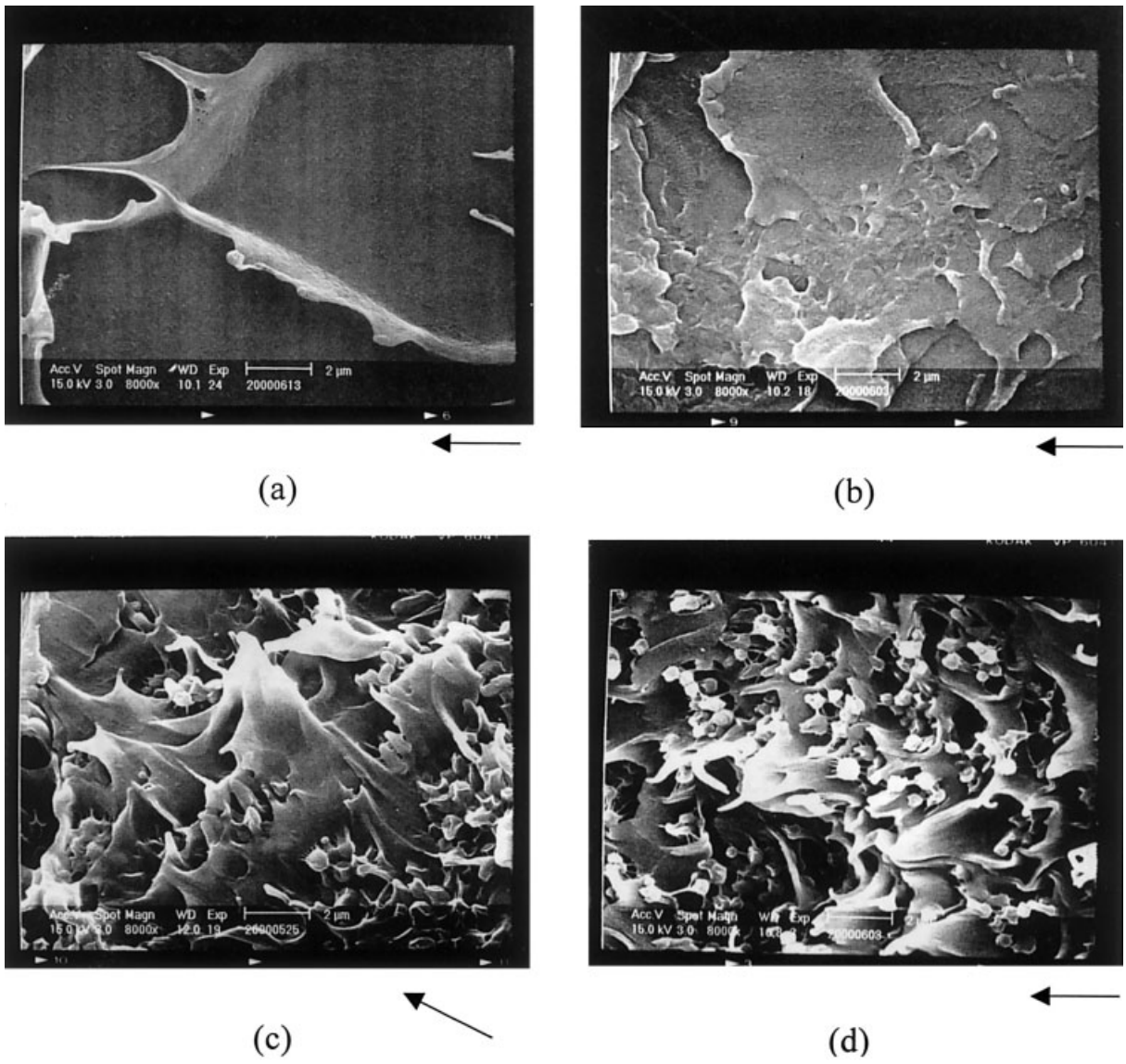

Figure 2 SEM photographs of the fracture surface by the Izod impact test: (a) PS, (b) MIL1, (c) MIL6, and (d) MIL10.

the top of the triangular phase diagram.[21] A lower M_n EVA delayed phase inversion of the mixture; thus, it was necessary to increase the conversion of SM to complete the phase inversion. If the phase conversion was not formed in the PS matrix, a lower M_n would cause poor tensile strength and impact strength.

Toughening mechanism

After the fracture surface of EVA-toughened PS was examined (see Figs. 1 and 2), some strips were extracted from the fracture surface in MIL1. All of the strips obviously connected one dispersed EVA particle to another, which was possibly caused by the craze formation in the interface of PS and EVA. Another energy absorption site was the EVA particle. The EVA particle could concentrate stress when an external stress was applied because the modulus of EVA was

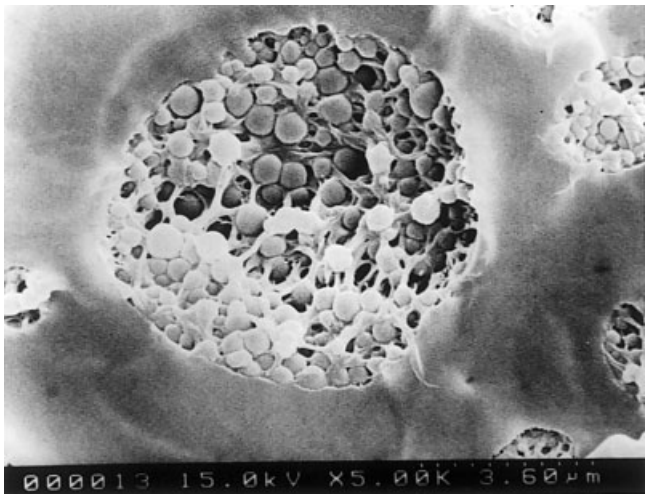

Figure 3 PS subinclusions enclosed within the EVA phase (MIL1).

lower than that of PS. Meanwhile, the maximum concentrated stress occurred near the equator of the dispersed particles, and the craze tip was formed around these particles. Thus, the PS matrix was locally deformed near the craze because stress was concentrated in the craze tip. Next, the ligaments and microvoids were formed by further strain. A ligament between two adjacent voids became stiff as the voids developed, tending to favor ligament deformation around adjacent, less well-developed voids. This stiffening led to the development of planar groups of voids, which acted effectively as cracks with ties formed by the ligaments across the surfaces. The cracks were formed until all the ligaments were ruptured. In the presence of EVA, multiple crazes occurred because the loading was dispersed by stress concentrator EVA particles. This could have also slowed the growth of craze to extend the strain and absorb more energy before fracture.

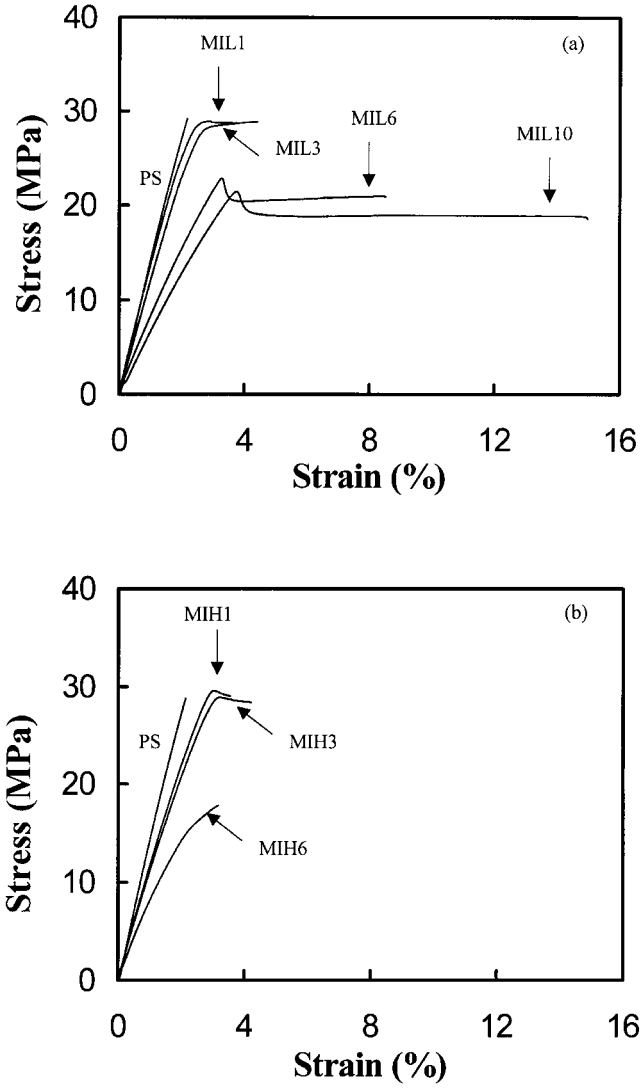

Figure 4 Tensile test curves of various EVA concentrations: MFI = (a) 0.7 and (b) 2.5.

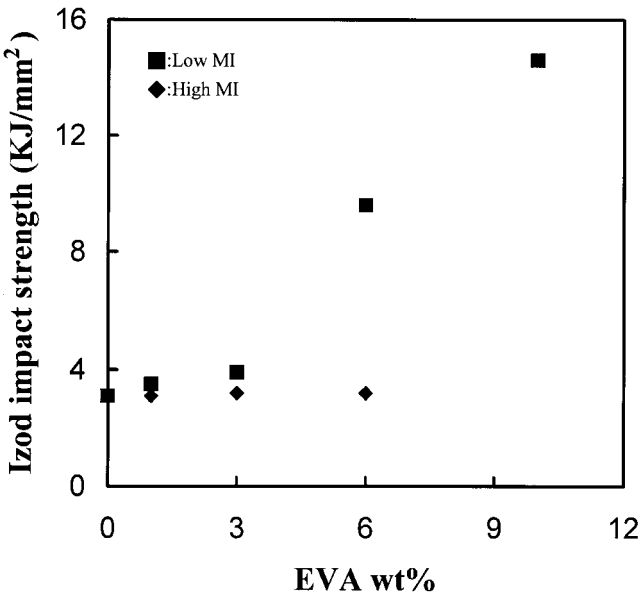

Figure 5 Results of the Izod impact strength test for different MFIs.

Moreover, crazes became fibril peaks at higher EVA concentrations. These fibril peaks were extracted from the fracture surface and were much longer than those in MIL1's toughened surface. Figure 6 shows that the PS matrix was deformed in the area around the EVA particles. The direction of deformation was parallel to the fracture surface, representing the presence of a shear band. No necking of the specimen was observed after examination of the volume change in the tensile test. Thus, shear yielding only occurred locally, and the fracture energy consumption effect was limited. However, this phenomenon depended on the amount of EVA particles and was, in fact, related to the distance between dispersed particles. A higher EVA concentration led to tightly packed particles; in other words, more overlapping stress fields increased the stress concentration and then seriously deformed the craze. Not only the PS matrix but also the EVA phase was deformed (Fig. 7). As shown in Figures 1, 6, and 7, the EVA phase with subinclusions of PS particles was dragged by stress to yield a fibril peaks fracture mechanism.

Consequently, the major toughening mechanisms were craze and the local deformation of PS. The deformation of EVA particles also absorbed part of the fracture energy but less than the former mechanisms. Thus, craze was the most important factor in the formation of EVA-toughened PS.

CONCLUSIONS

EVA was discovered to toughen PS in an SM polymerization system because the ethylene backbone in EVA is a good chain-transfer active site and PS-graft-

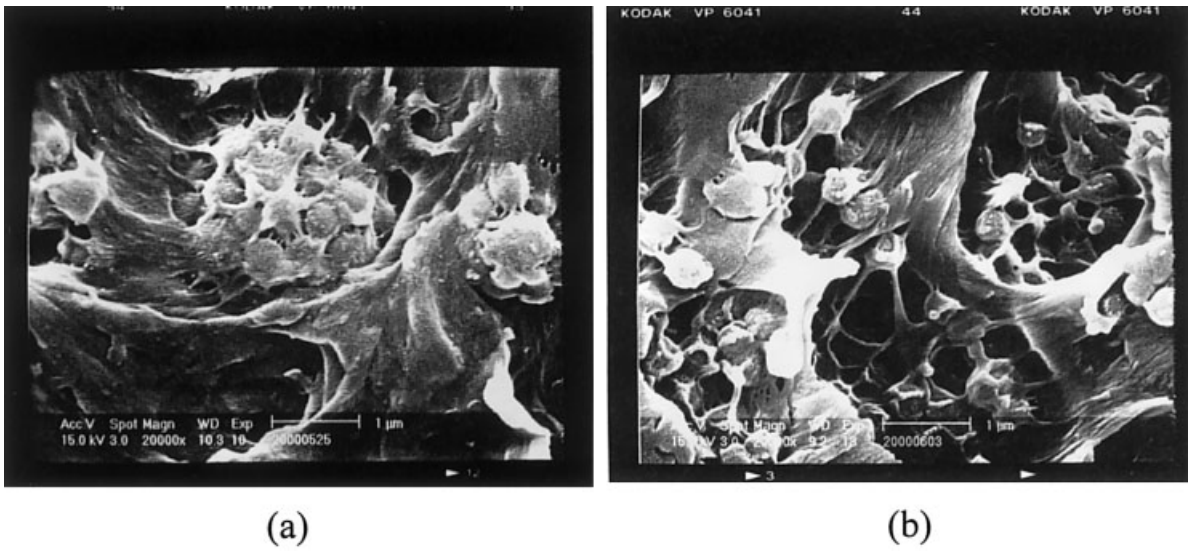

Figure 6 SEM photographs of the fracture surface near the EVA particle: (a) MIL6 and (b) MIL10.

ing EVA copolymerization occurred during SM polymerization. DSC results showed that the grafted PS chain influenced the crystallinity of EVA; thus, T_m, T_c, and X_c decreased. The fracture surfaces of EVA-toughened PS copolymer showed a large amount of craze when the concentration of EVA was 10%, and the impact strength was about five times that of pure PS. The elongation also increased by a factor of about six in MIL10, but the modulus was approximately halved. Additionally, the lower M_n of EVA delayed phase inversion, resulting in poor mechanical properties. When the tensile test results and SEM photos of the fracture surface were combined, the major mechanisms of EVA-toughened PS were shown to be craze and local matrix deformation.

Figure 7 SEM photograph of EVA deformation.

References

1. Amos, J. L.; McCurdy, J. L.; McIntire, O. R. U.S. Pat. 2,694,692 (1954).
2. Pohlemann, H. G.; Echte, A. Am Chem Soc Symp Ser 1981, 175, 265.
3. Polymer Microscopy, 2nd ed.; Sawyer, L. C.; Grubb, D. T., Eds.; Alden: Oxford, England, 1996; Chapter 4.
4. McCrum, N. G.; Buckley, C. P.; Bucknall, C. B. Principles of Polymer Engineering; Oxford University Press: Oxford, 1988.
5. Bucknall, C. B. In Comprehensive Polymer Science; Aggarwal, S., Ed.; Pergamon: Oxford University Press: Oxford, 1989; Vol. 7, Chapter 2.
6. Deanin, R. D.; Pickett, T. J.; Huang, J. C. Polym Mater Sci Eng 1989, 61, 950.
7. Soares, B. G.; Barbosa, R. V.; Covas, J. C. J Appl Polym Sci 1997, 65, 2141.
8. Barbosa, R. V.; Moraes, M. A. R.; Gomes, A. S.; Soares, B. G. Macromol Rep A 1995, 32 (Suppl. 5 and 6), 663.
9. Barbosa, R. V.; Soares, B. G.; Gomes, A. S. J Appl Polym Sci 1993, 47, 1411.
10. Barbosa, R. V.; Soares, M. G.; Gomes, A. S. Macromol Chem Phys 1994, 195, 3149.
11. Brydon, A.; Burnett, G. M.; Gameron, G. G. J Polym Sci Polym Chem Ed 1973, 11, 3255.
12. Brydon, A.; Burnett, G. M.; Gameron, G. G. J Polym Sci Polym Chem Ed 1974, 12, 1011.
13. Gameron, G. G.; Quereshi, M. Y. J Polym Sci Polym Chem Ed 1980, 18, 2143.
14. Gameron, G. G.; Quereshi, M. Y. J Polym Sci Polym Chem Ed 1980, 18, 3149.
15. Madhah, A. G.; Amin, M. B.; Usmani, A. M. Polym Bull 1985, 14, 433.
16. Alberts, H.; Bartl, H.; Kuhn. R. Adv Chem Ser 1975, 142, 214.
17. Choi, J. H.; Ahn, K. H.; Kim, S. Y. Polymer 2000, 21, 5229.
18. Goodier, J. N. Trans Am Soc Mech Eng 1933, 55, 39.
19. Michler, G. H.; Hamann, B.; Runge. Angew Makromol Chem 1990, 180, 106.
20. Thermodynamics of Polymer Solutions; Kurata, M., Ed.; Hardwood Academic: Chur, Switzerland, 1982; Vol. 1, Chapter 2.
21. Cheng, S. K.; Wang, C. C.; Chen, C. Y. J Polym Sci Part B: Polym Phys, to appear.